Mathematical modeling and dynamic analysis of anti-tumor immune response

Liuyong Pang[1] · **Sanhong Liu[2]** · **Xinan Zhang[3]** · **Tianhai Tian[4]**

Abstract

The competitive interaction of tumor-immune system is very complex. We aim to establish a simple and realistic mathematical model to understand the key factors that impact the outcome of an antitumor response. Based on the principle that lymphocytes undergo two stages of development (namely immature and mature), we develop a new anti-tumor-immune response model and investigate its property and bifurcation. The corresponding sufficient criteria for the asymptotic stabilities of equilibria and the existence of stable periodic oscillations of tumor levels are obtained. Theoretical results indicate that the system orderly undergoes different states with the flow rate of mature immune cells increasing, from the unlimited expansion of tumor, to the stable large tumor-present equilibrium, to the periodic oscillation, to the stable small tumor-present equilibrium, and finally to the stable tumor-free equilibrium, which exhibits a variety of dynamic behaviors. In addition, these dynamic behaviors are in accordance with some phenomena observed clinically, such as tumor dormant, tumor periodic oscillation, immune escape of tumor and so on. Numerical simulations are carried out to verify the results of our theoretical analysis.

Keywords Tumor-immune response · Qualitative analysis · Hopf bifurcation · Numerical simulations

✉ Liuyong Pang
  pangliuyong@163.com

✉ Xinan Zhang
  xinanzhang@mail.ccnu.edu.cn

1 School of Mathematics and Statistics, Huanghuai University, Zhumadian 463000, People's Republic of China

2 School of Mathematics and Statistics, Hubei University of Science and Technology, Xianning 437100, People's Republic of China

3 School of Mathematics and Statistics, Central China Normal University, Wuhan 430079, People's Republic of China

4 School of Mathematical Sciences, Monash University, Melbourne, VIC 3800, Australia

1 Introduction

According to the report of the World Health Organization, it was estimated that about 14 million cancer cases and 8.8 million cancer-related deaths in 2015. The number of new cases is expected to rise about 70% over the next 2 decades [1]. In particular, in China, about 4,292,000 new cancer cases diagnosed and 2,814,000 cancer deaths in 2015. Cancer remains the second most common cause of death, accounting for nearly 1 of every 4 deaths [2]. Hence, it is very important and requisite to find out the dynamic mechanism of initiation and development of tumor.

The growth of a cancerous tumor in vivo is a complicated process involving multiple biological interactions. In recent years, growing evidences have indicated that the immune system can recognize and eliminate malignant tumors [3,4]. The anti-tumor immune response begins when tumor cells are recognized as being alien. The cytotoxic T lymphocyte (CTL) are able to penetrate tumor parenchyma and recognize tumor-associated antigen, and correctly choose antigen for immunization. Hence, The tumor cells are killed by the cytotoxic T lymphocyte which can be found in all tissues in the body and in circulating blood stream [5]. Although much research has concentrated on how to strengthen the anti-tumor response by stimulating the immune system with vaccines or by direct injection of T cell or cytokines, the role of the immune system in the elimination of cancerous tissue is not fully understood [6–12].

To understand the interactions of immune system with tumor, many mathematical models have been established to investigate the tumor immune dynamics [13–23]. Bell applied the classic predator-prey interaction system to describe the response of effector cells to the growth of tumor cells [24]. Kuznetsov et al. [25] took into account the penetration of tumor cells by effector cells and presented a mathematical model of CTL cells response to the growth of immunogenic tumor, which exhibited a number of phenomena that were observed in vivo, including "sneaking through" and "dormant state" of the tumor. Moreover, the parameters of the targeted model were estimated by using the experimental data of chimeric mice. Pillis et al. [26–28] applied mathematical model to investigate the mechanisms of interaction between tumor cells and various immune effector cells, and applied the numerical calculations to discuss the treatment effects of different therapeutic regimens. Liu et al. [29] developed a mathematical model of tumor cells eliciting an immune response proposed by DeLisi and Rescigno [30] to investigate the dynamics of tumor and immune system interactions. Liu and Ruan made more realistic assumptions on model by requiring that lymphocytes go through two stages of development, namely immature and mature, and claimed that only lymphocytes in the second stage are effective in killing tumor cells. Our aim is to develop a simple and realistic mathematical model to reflect the phenomena observed clinically, and understand the key factors that impact the outcome of an antitumor response as clearly as possible.

The rest of the paper is organized as follows. A new model of ordinary differential equation is constructed to describe the interaction of tumor cell with T lymphocyte in Sect. 2. The qualitative and bifurcation analysis of the mathematical model are investigated in Sect. 3. Numerical simulations are carried out to illustrate the stability of equilibriums and the existence of stable periodic solution in Sect. 4. Finally, the conclusions are summarized in Sect. 5.

2 Construction of the mathematical model

In this paper, we follow the ideas of modelling immune reaction against the tumor presented by [29,30], and prefer to construct a simple but reasonable mathematical model to describe some phenomena observed clinically, such as immune escape of tumor, tumor dormant, periodic oscillations and so on. In order to facilitate the research, we denote the number of immature T lymphocytes, the number of mature T lymphocytes and the number of tumor cells as $L_1(t)$, $L_2(t)$ and $T(t)$, respectively, and make the following reasonable assumptions:

(a) A tumor admits an exponential growth model in the absence of an immune response. This is an accepted growth model for tumors, which is also able to fit and explain the tumor growth data [31]. The tumor growth rate is denoted by λ_2.

(b) Only mature T lymphocytes are capable of killing tumor cell [29,30]. The interaction term between tumor and the mature T lymphocytes takes the form of $\alpha_2 T L_2$, which is similar to a bilinear incidence rate in the epidemic dynamics, where α_2 is the rate of tumor cells killed by mature T lymphocytes.

(c) Inactivation of cytolytic potential occurs when the mature T lymphocytes have interacted with tumor cells several times and ceases to be effective [13]. We denote the inactivation rate of the mature T lymphocytes by α_3.

(d) The mature T lymphocytes are absolutely derived from the young lymphocytes. The transformation rate from the immature T lymphocytes to the mature T lymphocytes is λ_1.

(e) The immature T lymphocytes are normally present in the body, even when no tumor cells are present, since they are part of the innate immune response [32]. In the absence of tumor cells, the young lymphocytes can be produced at a fixed rate μ from hemopoietic system.

(f) Due to the presence of the tumor, the immature lymphocytes can be proliferated by the stimulation of tumor cells [25]. Moreover, by fitting experimental data, Kuznetsov and Taylor suggested that the recruitment term should be described by $\alpha_1 \frac{T L_2}{\eta + T}$, which is a Michaelis-Menten term, commonly used in anti-tumor immune response models to govern cell-to-cell interactions [5,15,27], where α_1 is the maximum recruitment rate.

From the above assumptions, the flowchart of model is depicted in Fig. 1. The transfer diagram leads to the following model:

$$\begin{cases} \frac{dL_1}{dt} = \mu - \lambda_1 L_1 + \alpha_1 \frac{T L_2}{\eta + T}, \\ \frac{dL_2}{dt} = \lambda_1 L_1 - \alpha_3 L_2, \\ \frac{dT}{dt} = \lambda_2 T - \alpha_2 T L_2, \end{cases} \tag{1}$$

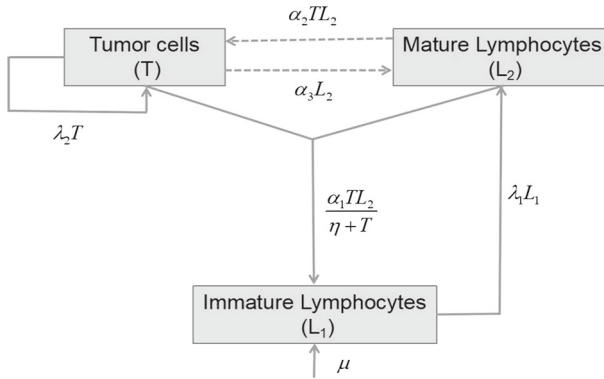To facilitate discussion, we denote $\mu = \lambda_0 L_0$. System (1) is rewritten as the following

Fig. 1 Flowchart of system (1)

$$\begin{cases} \frac{dL_1}{dt} = -\lambda_1(L_1 - \frac{\lambda_0}{\lambda_1}L_0) + \alpha_1\frac{TL_2}{\eta+T}, \\ \frac{dL_2}{dt} = \lambda_1 L_1 - \alpha_3 L_2, \\ \frac{dT}{dt} = \lambda_2 T - \alpha_2 T L_2, \end{cases} \qquad (2)$$

3 Qualitative and bifurcation analysis

3.1 Existence of equilibria

For the convenience of discussion, we make the following substitutions to simplify system (2). Substituting $L_1 - \frac{\lambda_0}{\lambda_1}L_0 = \frac{\alpha_1}{\alpha_2}x$, $L_2 = \frac{\lambda_1}{\alpha_2}y$, $T = \eta z$ and $t = \frac{1}{\lambda_1}\tau$, we have the corresponding simplified system

$$\begin{cases} \frac{dx}{d\tau} = -x + \frac{yz}{1+z}, \\ \frac{dy}{d\tau} = \alpha x - \beta y + \gamma, \\ \frac{dz}{d\tau} = \delta z - zy, \end{cases} \qquad (3)$$

where $\alpha = \frac{\alpha_1}{\lambda_1}$, $\beta = \frac{\alpha_3}{\lambda_1}$, $\gamma = \frac{\alpha_2\lambda_0}{\lambda_1^2}L_0$ and $\delta = \frac{\lambda_2}{\lambda_1}$.

It is easy to see that system (3) has two equilibria. In fact, the tumor-free equilibrium $E_1(0, \frac{\lambda}{\beta}, 0)$ always exists and the tumor-present equilibrium $E_2(\frac{\beta\delta-\gamma}{\alpha}, \delta, \frac{\beta\delta-\gamma}{\gamma+\alpha\delta-\beta\delta})$ exists if and only if $max\{0, (\beta-\alpha)\delta\} < \gamma < \beta\delta$. We can list the result in the following Table 1.

Next, we give some theoretical results of system (3).

3.2 Stability of equilibria

Theorem 1 *The tumor-free equilibrium E_1 is asymptotically stable if $\gamma > \beta\delta$, otherwise it is not stable.*

Table 1 Existence of equilibria

Conditions	Existence of equilibria
$0 < \beta < \alpha$	
$\quad 0 < \gamma < \beta\delta$	E_1, E_2
$\beta > \alpha > 0$	
$\quad 0 < \gamma < (\beta - \alpha)\delta$	E_1
$\quad (\beta - \alpha)\delta < \gamma < \beta\delta$	E_1, E_2
$\alpha, \ \beta > 0$	
$\quad \gamma > \beta\delta$	E_1

Fig. 2 The phase diagram of the system (3) shows that the tumor-free equilibrium E_1 is a saddle-focus point, where $\beta > \alpha$ and $0 < \gamma < (\beta - \alpha)\delta$
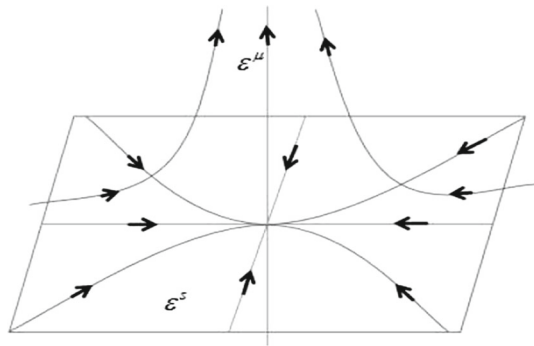
Proof The Jacobian matrix at E_1 of system (3) is

$$J(E_1) = \begin{bmatrix} -1 & 0 & \frac{\gamma}{\beta} \\ \alpha & -\beta & 0 \\ 0 & 0 & \delta - \frac{\gamma}{\beta} \end{bmatrix}.$$

The characteristic equation of $J(E_1)$ is

$$f(\lambda) = (\lambda + 1)(\lambda + \beta)[\lambda - (\delta - \frac{\gamma}{\beta})] = 0.$$

Obviously, the eigenvalues of $J(E_1)$ are

$$\begin{cases} \lambda_1 = -1, \\ \lambda_2 = -\beta, \\ \lambda_3 = -\frac{\gamma - \beta\delta}{\beta}, \end{cases}$$

respectively. Clearly, all these eigenvalues are negative when $\gamma > \beta\delta$. Therefore, the tumor-free equilibrium E_1 is locally asymptotically stable if $\gamma > \beta\delta$ and unstable if $\gamma < \beta\delta$. □

Remark When $\beta > \alpha$ and $0 < \gamma < (\beta - \alpha)\delta$, system (3) only has one equilibrium, i.e., a tumor-free equilibrium E_1. In addition, $J(E_1)$ has two negative eigenvalues and

one positive eigenvalue, then the tumor-free equilibrium E_1 is unstable. In this case, the tumor-free equilibrium E_1 is a saddle-focus point with a stable two-dimensional subspace ε^s and an unstable one-dimensional subspace ε^u. Hence, from Fig. 2, we know that $\lim\limits_{t\to+\infty} z(t) \to +\infty$ [33].

In order to investigate the stability of the tumor-present equilibrium E_2, we discuss the following two cases:

(I) The first case: $\beta < \alpha$

In this case, the existing condition of E_2 is $0 < \gamma < \beta\delta$.

Theorem 2 *The tumor-present equilibrium E_2 is locally asymptotically stable if $\gamma_1^* < \gamma < \beta\delta$ and unstable if $0 < \gamma < \gamma_1^*$. Wherein, γ_1^* is the only positive root of the equation*

$$f(\gamma) = \gamma^2 + (\alpha + \alpha\beta + \alpha\delta - 2\beta\delta)\gamma + \beta(\beta - \alpha)\delta^2 = 0. \tag{4}$$

Proof The Jacobian matrix of system (3) at E_2 is

$$J(E_2) = \begin{bmatrix} -1 & \frac{z_2}{1+z_2} & \frac{y_2}{(1+z_2)^2} \\ \alpha & -\beta & 0 \\ 0 & -z_2 & 0 \end{bmatrix}.$$

The characteristic equation of system (3) is given by

$$g(\lambda) = \lambda^3 + A_1\lambda^2 + A_2\lambda + A_3 = 0, \tag{5}$$

where

$$\begin{aligned} A_1 &= 1 + \beta, \\ A_2 &= \frac{\gamma}{\delta}, \\ A_3 &= \frac{(\beta\delta - \gamma)(\gamma - \beta\delta + \alpha\delta)}{\alpha\delta}, \\ A_1 A_2 - A_3 &= \frac{\alpha\gamma(1+\beta) - (\beta\delta - \gamma)(\gamma - \beta\delta + \alpha\delta)}{\alpha\delta} \\ &= \frac{\gamma^2 + (\alpha + \alpha\beta + \alpha\delta - 2\beta\delta)\gamma + \beta(\beta - \alpha)\delta^2}{\alpha\delta} \\ &= \frac{f(\gamma)}{\alpha\delta} \end{aligned} \tag{6}$$

It is clear that $A_1 > 0$, $A_2 > 0$, $A_3 > 0$ if $0 < \gamma < \beta\delta$ and $\beta < \alpha$. Since $f(0) = \beta(\beta - \alpha)\delta^2 < 0$ and $f(\beta\delta) = \alpha(1+\beta)\beta\delta > 0$, the characteristic equation of system (3) has only one positive root which is denoted by γ_1^*. Clearly, $\gamma_1^* < \beta\delta$. In addition, $f(\gamma) > 0$ when $\gamma_1^* < \gamma < \beta\delta$, which admits $A_1 A_2 - A_3 > 0$ (see Fig. 3). Therefore, the tumor-present equilibrium E_2 is locally asymptotically stable if $\gamma_1^* < \gamma < \beta\delta$ and unstable if $0 < \gamma < \gamma_1^*$.   □

(II) The second case: $\beta > \alpha$

Fig. 3 The figure of the quadratic function $f(\gamma)$, where $\beta < \alpha$
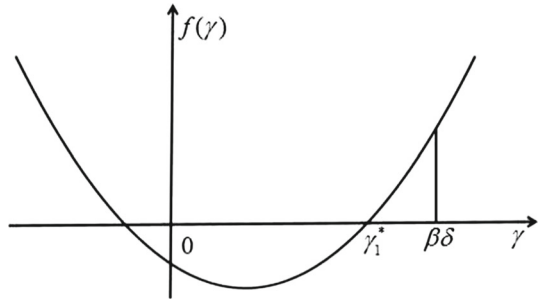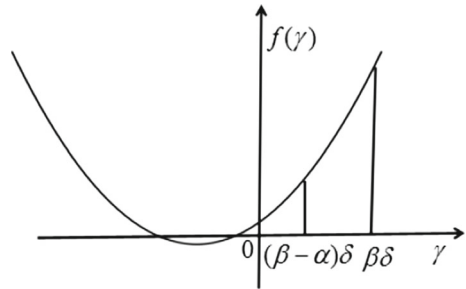

Fig. 4 The figure of the quadratic function $f(\gamma)$, where $\beta > \alpha$ and $\delta^* > \delta$

Obviously, E_2 exists only when $(\beta - \alpha)\delta < \gamma < \beta\delta$ and the characteristic equation of system (3) is (5). Similarly, we know that A_1, A_2, $A_3 > 0$ and the sign of $A_1 A_2 - A_3$ is determined by the sign of $f(\gamma)$. We need to ascertain the sign of $f(\gamma)$.

From Eq. (4), we have

$$f((\beta - \alpha)\delta) = \alpha(1 + \beta)(\beta - \alpha)\delta > 0,$$
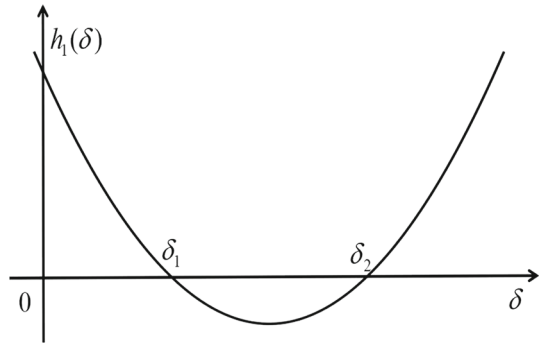$$f(\beta\delta) = \alpha(1 + \beta)\beta\delta > 0.$$

For the sake of convenience, we note $\delta^* \triangleq \frac{\alpha(1+\beta)}{2\beta-\alpha}$. In the following, we take into account two cases:

(1) When $0 < \delta \leq \delta^*$, i.e., $\alpha + \alpha\beta + \alpha\delta - 2\beta\delta \geq 0$, the symmetry axis of the quadratic function $f(\gamma)$ locates at the left-hand side of the curve $\gamma = 0$ or is just the curve $\gamma = 0$. When $(\beta - \alpha)\delta < \gamma < \beta\delta$, $f(\gamma) > 0$ is always correct (see Figure 4).
(2) When $\delta > \delta^*$, i.e., $\alpha + \alpha\beta + \alpha\delta - 2\beta\delta < 0$, the symmetry axis of the quadratic function (4) lies on the right-hand side of the curve $\gamma = 0$.

From the discriminant of the quadratic equation $f(\gamma) = 0$, we have

$$
\begin{aligned}
h_1(\delta) &= (\alpha + \alpha\beta + \alpha\delta - 2\beta\delta)^2 - 4\beta(\beta - \alpha)\delta^2 \\
&= \alpha[\alpha + \alpha\beta^2 + \alpha\delta^2 + 2\alpha\beta + 2\alpha\delta + 2\alpha\beta\delta - 4\beta\delta - 4\beta^2\delta] \\
&= \alpha^2\delta^2 + 2[\alpha^2(1 + \beta) - 2\alpha\beta(1 + \beta)]\delta + \alpha^2(1 + \beta)^2 \\
&= \alpha^2\delta^2 + 2(1 + \beta)(\alpha - 2\beta)\alpha\delta + \alpha^2(1 + \beta)^2.
\end{aligned}
\tag{7}
$$

Then,

$$
\begin{aligned}
h_1(\delta^*) &= \frac{\alpha^4(1+\beta)^2}{(2\beta-\alpha)^2} - 2\alpha^2(1+\beta)^2 + \alpha^2(1+\beta)^2 \\
&= \alpha^2(1+\beta)^2[\frac{\alpha^2}{(\beta-\alpha)^2} - 1] \\
&= \frac{4\alpha^2\beta(1+\beta)^2}{2\beta-\alpha}(\alpha-\beta) < 0.
\end{aligned}
\tag{8}
$$

In addition, from the discriminant of the quadratic equation $h_1(\delta) = 0$

$$
\begin{aligned}
\Delta &= 4(1+\beta)^2\alpha^2(\alpha-2\beta)^2 - 4\alpha^4(1+\beta)^2 \\
&= 4\alpha^2(1+\beta)^2[\alpha^2 - 4\alpha\beta + 4\beta^2 - \alpha^2] \\
&= 16\beta\alpha^2(1+\beta)^2(\beta-\alpha) > 0,
\end{aligned}
\tag{9}
$$

we know that the quadratic equation $h_1(\delta) = 0$ has two roots

$$
\begin{aligned}
\delta_1 &= \frac{(1+\beta)[2\beta-\alpha-\sqrt{\beta(\beta-\alpha)}]}{\alpha} \\
\delta_2 &= \frac{(1+\beta)[2\beta-\alpha+\sqrt{\beta(\beta-\alpha)}]}{\alpha}.
\end{aligned}
$$

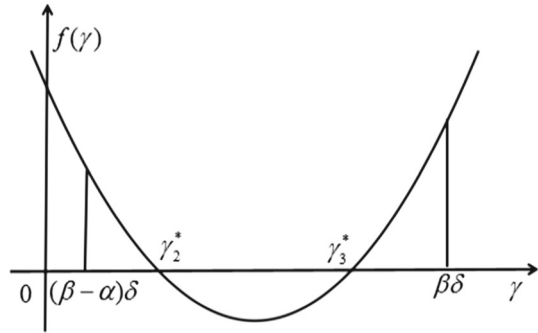Obviously, $\delta_1 < \delta^* < \delta_2$. We know that $h_1(\delta) < 0$ if $\delta^* < \delta < \delta_2$ (see Fig. 5), then
$f(\gamma) > 0$. Hence, we can give the following result:

Theorem 3 *The tumor-present equilibrium E_2 is locally asymptotically stable if $\beta >$
α, $0 < \delta < \delta_2$ and $(\beta - \alpha)\delta < \gamma < \beta\delta$.*

Furthermore, if $\delta > \delta_2$, $h_1(\delta) > 0$. Then, the equation $f(\gamma) = 0$ has two positive
roots at the interval $[(\beta - \alpha)\delta, \beta\delta]$

$$
\gamma_2^* = \frac{2\beta\delta - \alpha - \alpha\beta - \alpha\delta - \sqrt{h_1(\delta)}}{2}, \quad \gamma_3^* = \frac{2\beta\delta - \alpha - \alpha\beta - \alpha\delta + \sqrt{h_1(\delta)}}{2}.
$$

Obviously, when $\beta > \alpha$, $\delta > \delta_2$, we have $(\beta - \alpha)\delta < \gamma_2^* < \gamma_3^* < \beta\delta$. Furthermore, $f(\gamma) > 0$ if $\gamma \in ((\beta - \alpha)\delta, \gamma_2^*)$ or $\gamma \in (\gamma_3^*, \beta\delta)$ and $f(\gamma) < 0$ if $\gamma \in (\gamma_2^*, \gamma_3^*)$ and $f(\gamma) = 0$ if $\gamma = \gamma_2^*$ or $\gamma = \gamma_3^*$ (see Fig. 6). Hence, we can draw the conclusion as follows.

Theorem 4 *If $\beta > \alpha$ and $\delta > \delta_2$, the tumor-present equilibrium E_2 is locally asymptotically stable when $\gamma \in ((\beta - \alpha)\delta, \gamma_2^*)$ or $\gamma \in (\gamma_3^*, \beta\delta)$ and unstable when $\gamma_2^* < \gamma < \gamma_3^*$.*

3.3 Analysis of hopf bifurcation

From Theorem 2, we know that if $\gamma = \gamma_1^*$, i.e., $A_1 A_2 - A_3 = 0$, $J(E_2)$ has one negative eigenvalue $\lambda = -A_1$ and two purely imaginary eigenvalues $\lambda_{2,3} = \pm\omega i$ (where $\omega = \sqrt{A_2} > 0$), which suggests that system (3) may undergoes a Hopf bifurcation around the equilibrium E_2. Here, we explore the existence of the Hopf bifurcation. First of all, we quote a useful lemma [34–37].

Lemma 1 *Let $\Omega \in \mathbb{R}^3$ be an open set containing $O(x_1, x_2, x_3)$ and let $S \subseteq \mathbb{R}$ be an open set with $0 \in S$. Let $f : \Omega \times S \to \mathbb{R}^3$ be an analytic function such that $f(0, \rho) = 0$ for any $\rho \in S$. Assume that the variational matrix $Df(0, \rho)$ of f has one real eigenvalue $\gamma(\rho)$ and two conjugate imaginary eigenvalues $\alpha(\rho) \pm i\beta(\rho)$ with $\gamma(0) < 0$, $\alpha(0) = 0$, $\beta(0) > 0$. Furthermore, suppose that the eigenvalues cross the imaginary axis with nonzero speed, that is, $\frac{d\alpha(0)}{d\rho} \neq 0$. Then the following differential system*

$$\dot{X} = f(X, \rho)$$

undergoes a Hopf bifurcation near the equilibrium point O at $\rho = 0$.

Here we choose the intrinsic growth rate γ as the perturbation parameter. Without loss of generality, we set $\gamma(\rho) = \gamma_1^* + \rho$, where $\gamma(0) = \gamma_1^*$ satisfies that $(A_1 A_2 - A_3)|_{\rho=0} = 0$. We also need to determine the sign of the real part of $\frac{d\lambda}{d\rho}$ at $\rho = 0$ when the above equation is valid. Differentiating Eq. (5) with respect to ρ, we have

$$3\lambda^2 \frac{d\lambda}{d\rho} + 2A_1\lambda\frac{d\lambda}{d\rho} + \frac{1}{\delta}\lambda + A_2\frac{d\lambda}{d\rho} + \frac{-(2\gamma - 2\beta\delta + \alpha\delta)}{\alpha\delta} = 0. \qquad (10)$$

which leads to

$$\frac{d\lambda}{d\rho} = -\frac{\alpha\lambda - (2\gamma - 2\beta\delta + \alpha\delta)}{\alpha\delta(3\lambda^2 + 2A_1\lambda + A_2)}. \tag{11}$$

Thus

$$
\begin{aligned}
V_c &= sign\{-Re(\frac{d\gamma}{d\rho}|_{\rho=0})\} \\
&= sign\{-Re(\frac{\alpha\omega i - (2\gamma - 2\beta\delta + \alpha\delta)}{\alpha\delta(-3A_2 + 2A_1\omega i + A_2)}|_{\gamma=\gamma_1^*})\} \\
&= sign\{-Re(\frac{\alpha\omega i - (2\gamma - 2\beta\delta + \alpha\delta)}{-A_2 + A_1\omega i}|_{\gamma=\gamma_1^*})\} \\
&= sign\{-[2\gamma + \alpha(1 + \beta) + \alpha\delta - 2\beta\delta]|_{\gamma=\gamma_1^*}\} \\
&= sign\{-\frac{df(\gamma)}{d\gamma}|_{\gamma=\gamma_1^*}\} \\
&= -1,
\end{aligned}
$$

which also can be seen from Fig. 3. Hence, we have the following result:

Theorem 5 *If $\beta < \alpha$ and $\gamma = \gamma_1^*$, system (3) undergoes a non-degenerate Hopf bifurcation at the tumor-present equilibrium E_2.*

From the proof of Theorem 4, $A_1A_2 - A_3 = 0$ if $\gamma = \gamma_2^*$ or $\gamma = \gamma_3^*$. Similarly, we know that $J(E_2)$ has one negative eigenvalue $\lambda = -A_1$ and two purely imaginary eigenvalues $\lambda_{2,3} = \pm\omega i$ (where $\omega = \sqrt{A_2} > 0$). Through the same calculation process, we know that when $\gamma = \gamma_2^*$, transversality condition $V_C = -1$, and when $\gamma = \gamma_3^*$, transversality condition $V_C = -1$. Hence, we have

Theorem 6 *If $\alpha < \beta$, $\delta > \delta_2$ and $\gamma = \gamma_2^*$ or $\gamma = \gamma_3^*$, system (3) undergoes a non-degenerate Hopf bifurcation at the tumor-present equilibrium E_2.*

The results of Theorems 1–6 are listed in Table 2.

4 Numerical simulations

In this section, we will choose suitable parameters of system (3) to numerically validate the theoretical conclusions obtained in the previous sections. Without loss of generality, we only present numerical results of the second case (i.e., $\beta > \alpha$). We take the values of α and β as 0.3 and 0.6, respectively. By calculating, we obtain $\delta_2 = 9.325$. Hence, we take $\delta = 10 > \delta_2$, then the quadratic equation $f(\gamma) = 0$ have two positive roots, i.e., $\gamma_2^* = 3.88$ and $\gamma_3^* = 4.64$. Moreover, $(\beta - \alpha)\delta = 3$ and $\beta\delta = 6$. Next, we will apply the results of numerical simulation to exhibit the variation rules of system states with the normal flow rate of T lymphocyte γ increasing, and to illustrate some biological phenomena observed clinically.

1. Choose $\alpha = 0.3$, $\beta = 0.6$, $\delta = 10$ and $\gamma = 2$, then $\gamma < (\beta - \alpha)\delta$. Hence, from Theorem 1 and Remark, we know that the tumor-free equilibrium E_1 is a saddle-focus point. Hence, the number of tumor cells goes to infinity (see Fig. 7).

Table 2 Properties of equilibria

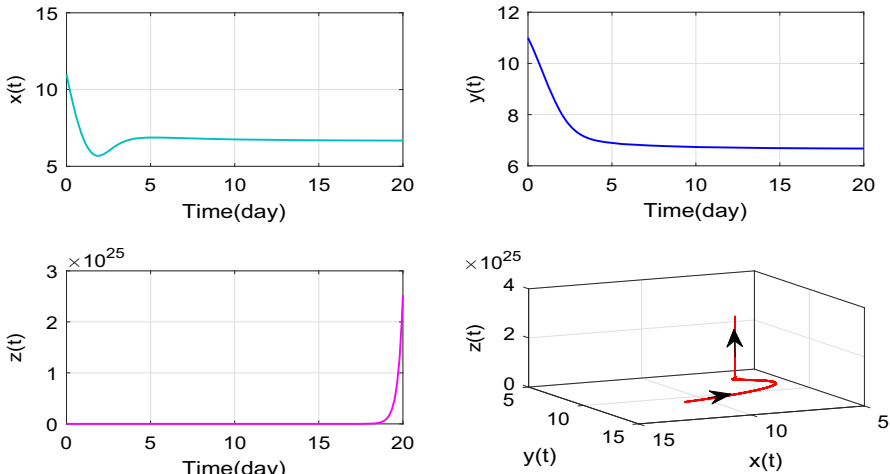| Conditions	Properties of equilibria	
	E_1	E_2
$0 < \beta < \alpha$		
$\quad 0 < \gamma < \gamma_1^*$	Unstable	Unstable
$\quad \gamma_1^* < \gamma < \beta\delta$	Unstable	Stable
$\quad \gamma = \gamma_1^*$	Unstable	Hopf bifurcation
$\beta > \alpha > 0$		
$\quad 0 < \gamma < (\beta - \alpha)\delta$	Unstable	Inexistence
$\quad 0 < \delta < \delta_2$		
$\qquad (\beta - \alpha)\delta < \gamma < \beta\delta$	Unstable	Stable
$\quad \delta > \delta_2$		
$\qquad (\beta - \alpha)\delta < \gamma < \gamma_2^*$	Unstable	Stable
$\qquad \gamma_2^* < \gamma < \gamma_3^*$	Unstable	Unstable
$\qquad \gamma_3^* < \gamma < \beta\delta$	Unstable	Stable
$\qquad \gamma = \gamma_2^* \text{ or } \gamma = \gamma_3^*$	Unstable	Hopf bifurcation
$\alpha,\ \beta > 0$		
$\quad \gamma > \beta\delta$	Stable	Inexistence

Fig. 7 The figure indicates that the number of tumor cells increases without restriction, which is in accord with the immune escape phenomena of tumor observed clinically, where $\alpha = 0.3$, $\beta = 0.6$, $\gamma = 2$, $\delta = 10$

2. Choose $\alpha = 0.3$, $\beta = 0.6$, $\delta = 10$ and $\gamma = 3.5$, then $(\beta - \alpha)\delta < \gamma < \gamma_2^* \Rightarrow f(\gamma) > 0$. Hence, from Theorem 3, we know that the large tumor-present equilibrium E_2 is asymptotically stable (see Fig. 8).

3. Choose $\alpha = 0.3$, $\beta = 0.6$, $\delta = 10$ and $\gamma = 4$, then $\gamma_2^* < \gamma < \gamma_3^* \Rightarrow f(\gamma) < 0$. Hence, from Theorem 6, we know that a limit cycle will bifurcate from the tumor-
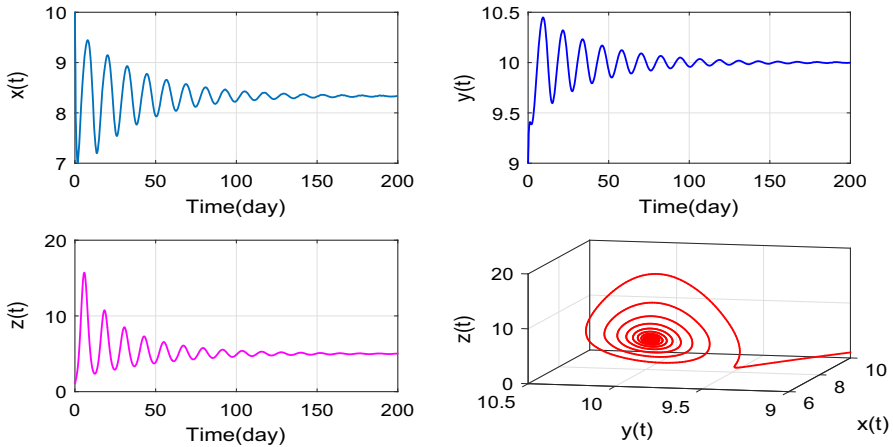
Fig. 8 The figure exhibits the large tumor-present equilibrium E_2 is asymptotically stable,which is lined with the state of the dormancy tumor observed clinically and means that the level of the tumor cells does not change, where $\alpha = 0.3$, $\beta = 0.6$, $\gamma = 3.5$, $\delta = 10$
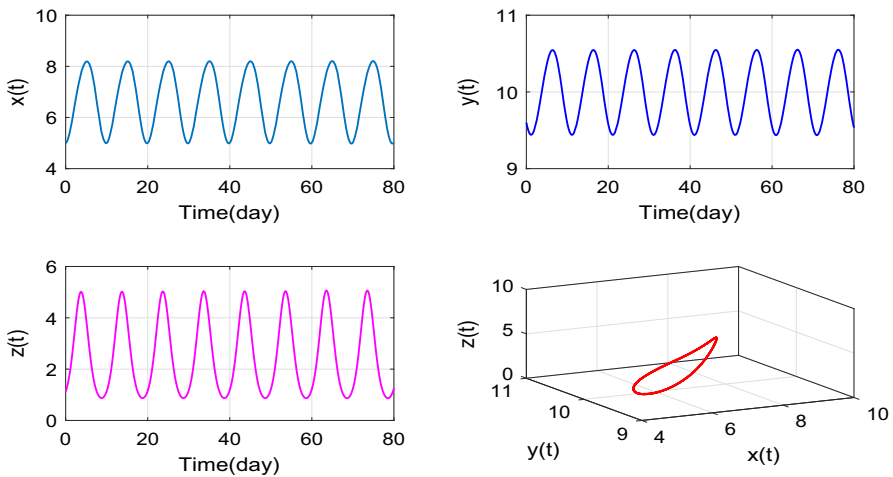

Fig. 9 The figure shows that system (3) occurs a periodic orbit around E_2, which in accord with the oscillatory phenomena in tumors observed clinically, where $\alpha = 0.3$, $\beta = 0.6$, $\gamma = 4$, $\delta = 10$

present equilibrium E_2 by perturbing the value of parameters γ near 4.64, which indicates that a periodic orbit of system (3) occurs at E_2 (see Fig. 9).

4. Choose $\alpha = 0.3$, $\beta = 0.6$, $\delta = 10$ and $\gamma = 5$, then $\gamma_3^* < \gamma < \beta\delta \Rightarrow f(\gamma) > 0$. Hence, from Theorem 4, we know that the small tumor-present equilibrium E_2 is asymptotically stable (see Fig. 10).

5. Choose $\alpha = 0.3$, $\beta = 0.6$, $\gamma = 6.2$, $\delta = 10$, then it is easy to know $\gamma > \beta\delta$. From Theorem 1, we know that the tumor-free equilibrium E_1 is asymptotically stable (see Fig. 11).
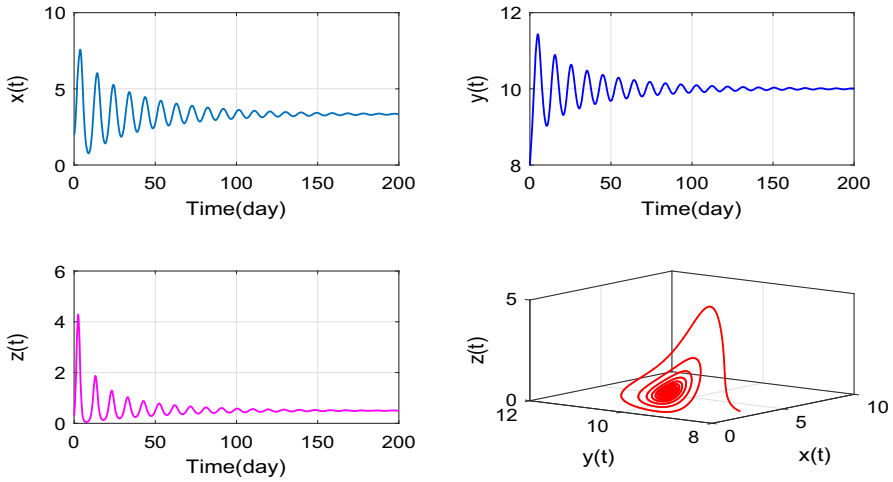
Fig. 10 The figure illuminates the small tumor-present equilibrium E_2 is asymptotically stable, which is in accord with the state of the dormancy tumor observed clinically and means that the level of the tumor cells does not change [25], where $\alpha = 0.3$, $\beta = 0.6$, $\gamma = 5$, $\delta = 10$ respectively
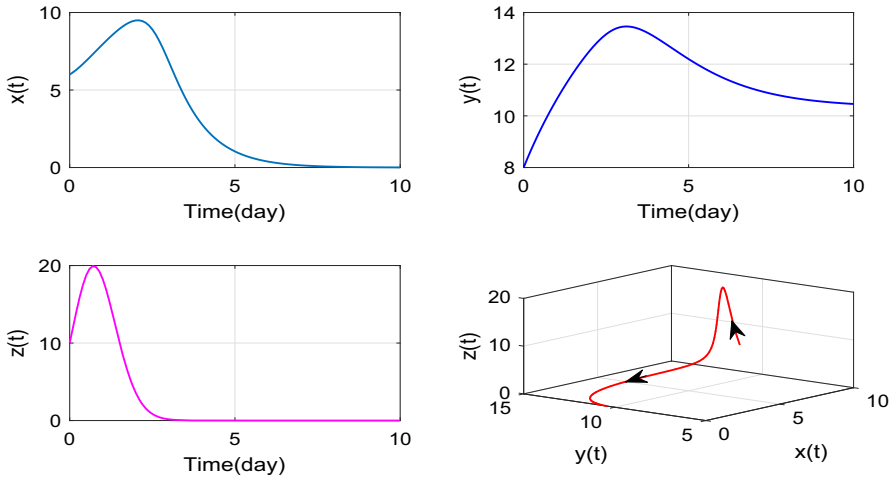

Fig. 11 The figure clarifies the tumor-free equilibrium E_1 is asymptotically stable if parameters are taken as $\alpha = 0.3$, $\beta = 0.6$, $\gamma = 0.6$, $\delta = 0.8$, which is in accord with the spontaneous tumor regression phenomena observed clinically

5 Discussion

In this paper, choosing γ as key parameter, we proposed a two-stage model of tumor immune response and studied the effect of immune system on inhibiting tumor growth based on the mechanism and characteristics of anti-tumor immune response. Two cases are discussed to investigate the dynamic behavior of system (3).

Fig. 12 For $\beta < \alpha$, the figure exhibits the rules of variation of system states with the normal flow rate of T lymphocyte γ increasing
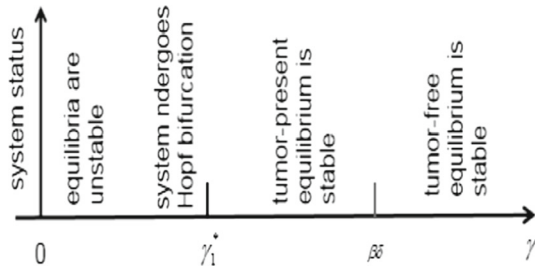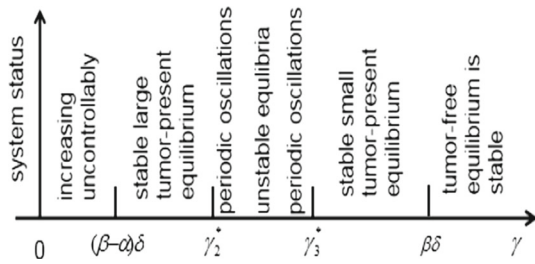

Fig. 13 For $\beta > \alpha$, the figure represents the rules of variation of system states with the normal flow rate of T lymphocyte γ increasing

For the first case (i.e., $\beta < \alpha$), the states of system (3) successively undergo several changes, from unstable equilibria, to periodic oscillation, to the stable tumor-present equilibrium and to the stable tumor-free equilibrium (see Fig. 12). In other word, in consistent with oscillatory growth phenomena of tumors observed clinically, the number of tumor cells exhibits periodic oscillation when the strength of the immune response to tumor is relatively weak, and the immune cells and tumor cells will reach a positive equilibrium state as the anti-tumor immune response strengthens. Furthermore, the tumor will be eventually eliminated only if the normal flow rate of immune cells become stronger (i.e., $\gamma > \beta\delta$).

For another case (i.e., $\beta > \alpha$), we obtain more plentiful kinetic properties (see Fig. 13). In this case ,we obtain four threshold values of the normal flow rate of immune cells γ, which are $(\beta - \alpha)\delta$, γ_2^*, γ_3^* and $\beta\delta$, respectively. When the normal rate of flow of immune cells γ is less than threshold value $(\beta - \alpha)\delta$, the tumor cells will increase uncontrollably, which indicates that tumors development are not controlled by the immune system any longer, which in accord with immune escape phenomena observed clinically (see Fig. 7). When the flow rate of immune cells γ is in between $(\beta - \alpha)\delta$ and γ_2^*, a large tumor-present equilibrium is stable (see Fig. 8). The tumor dormancy phenomena can be observed by numerical simulation. Furthermore, when parameter value γ is in the interval $[\gamma_2^*, \gamma_3^*]$, system (3) brings birth a periodic orbit (see Fig. 9), which indicates that the number of tumor cells will exhibit periodic oscillations. As the parameter value γ increase continually (i.e., $\gamma \in (\gamma_3^*, \beta\delta)$), a small tumor-present equilibrium is stable (see Fig. 10). Finally, when the normal rate of flow of immune cells γ is more than threshold value $\beta\delta$, the tumor will be ultimately extinct (see Fig. 11). It can be seen that our results are quite realistic.

Although the mathematical model is simple, the system exhibits rich dynamic properties, which can make some phenomena observed clinically very clear, such as immune escape of tumor, tumor dormant, oscillatory growth patterns in tumors,

spontaneous tumor regression and so on. Numerical simulations are carried out to verify the results of our theoretical analysis.

References

1. World Health Organization: Media centre, Cancer http://www.who.int/mediacentre/factsheets/fs297/en/
2. Chen, W., Zheng, R., Baade, P., et al.: Cancer statistics in China, 2015. CA Cancer J. Clin. **66**, 115–132 (2016)
3. Parish, C.: Cancer immunotherapy: the past, the present and the future. Immunol. Cell Biol. **81**, 106–113 (2003)
4. Smyth, M., Godfrey, D.: A fresh look at tumor immunosurveillance and immunotherapy. Nat. Immunol. **2**, 293–299 (2001)
5. Galach, M.: Dynamics of the tumor-immune system competition-the effect of time delay. Int. J. Appl. Math. Comput. Sci. **13**, 395–406 (2003)
6. Raluca, E., Bramson, J., Earn, D.: Interactions between the immune system and cancer: a brief review of non-spatial mathematical models. Bull. Math. Biol. **73**, 2–23 (2011)
7. Rosenberg, S., Yang, J., Restifo, N.: Cancer immunotherapy: moving beyond current vaccines. Nat. Med. **10**, 909–915 (2004)
8. Riddell, S.: Progress in cancer vaccines by enhanced self-presentation. Proc. Natl. Acad. Sci. USA **98**, 8933–8935 (2001)
9. Hirayama, M., Nishimur, Y.: The present status and future prospects of peptide-based cancer vaccines. Int. Immunol. **28**, 319–328 (2016)
10. Scott, A., Wolchok, J.: Antibody therapy of cancer. Nat. Rev. **12**, 278–287 (2012)
11. Pincetic, A., Bournazos, S., DiLillo, D., et al.: Type I and type II Fc receptors regulate innate and adaptive immunity. Nat. Immunol. **15**, 707–16 (2014)
12. Weiner, L., Surana, R., Wang, S.: Monoclonal antibodies: versatile platforms for cancer immunotherapy. Nat. Rev. **10**, 317–27 (2010)
13. Adam, J., Bellomo, T.: Survey of models for tumor-immune system dynamics. Birkhauser, Boston (1997)
14. Chaplain, M., Matzavions, A.: Mathematical modeling of spation-temporal phenomena in tumor immunology. Tutor. Math. Biosci. **3**, 131–183 (2006)
15. Kirschner, D., Panetta, J.: Modeling immunotherapy of the tumor-immune interaction. J. Math. Biol. **37**, 235–252 (1998)
16. Mallet, D., Pillis, L.: A cellular automata model of tumor-immune system interactions. J. Theor. Biol. **239**, 334–350 (2006)
17. d'Onofrio, A.: A general framework for modeling tumor-immune system competition and immunotherapy: mathematical analysis and biomedical inferences. Physica D **208**, 220–235 (2005)
18. Kirschner, D., Tsygvintsev, A.: On the global dynamics of a model for tumor immunotherapy. Math. Biosci. Eng. **6**, 573–583 (2009)
19. Pang, L., Zhao, Z., Hong, S.: Dynamic analysis of an antitumor model and investigation of the therapeutic effects for different treatment regimens. Comput. Appl. Math. **36**, 537–560 (2017)
20. Lejeune, O., Chaplain, M., Akili, I.: Oscillations and bistability in the dynamics of cytotoxic reactions mediated by the response of immune cells to solid tumours. Math. Comput. Model. **47**, 649–662 (2008)
21. Pang, L., Zhao, Z., Song, X.: Cost-effectiveness analysis of optimal strategy for tumor treatment. Chaos Solitions Fractals **87**, 293–301 (2016)

22. Pang, L., Shen, L., Zhao, Z.: Mathematical modeling and analysis of the tumor treatment regimens with pulsed immunotherapy and chemotherapy. Comput. Math. Methods Med. **2016**, 1–12 (2016)
23. Kuznetsov, V.A., Zhivoglyadov, V.P., Stepanova, L.A.: Kinetic approach and estimation of parameters of cellular interaction between immunity system and a tumor. Arch. Immunol. Ther. Exp. **2**, 465–476 (1992)
24. Bell, G.I.: Predator–prey equations simulating an immune response. Math. Biosci. **16**, 291–314 (1973)
25. Kuznetsov, V.A., Makalkin, L.A., Talor, M.A., perelson, A.S.: Nonlinear dynamics of immunogenic tumors: parameter estimation and global bifurcation analysis. Bull. Math. Biol. **56**, 295–321 (1994)
26. de Pillis, L.G., Radunskaya, A.E., Wiseman, C.L.: A validated mathematical model of cell-mediated immune response to tumor growth. Cancer Res. **65**, 7950–7958 (2005)
27. de Pillis, L.G., Radunskaya, A.: A mathematical tumor model with immune resistance and drug therapy : an optimal control approach. J. Theor. Med. **3**, 79–100 (2000)
28. de Pillis, L.G., Fister, K.Renee, et al.: Mathematical model creation for cancer chemo-immuntherapy. Comput. Math. Methods Med. **10**, 165–184 (2009)
29. Liu, D., Ruan, S., Zhu, D.: Stable periodic oscillations in a two-stage cancer model of tumor and immune system interactions. Math. Biosci. Eng. **9**, 347–368 (2012)
30. DeLisi, C., Rescigno, A.: Immune surveillance and neoplasia-I: a minimal mathematical model. Bull. Math. Biol. **39**, 201–221 (1977)
31. Skipper, H., Schabel, F.: Quantitative and cytokinetic studies in experimental tumor systems. Cancer Med. **2**, 636–648 (1982)
32. Roitt, I., Brostoff, J., Male, D.: Immunology. Mosby, St. Louis (1993)
33. Shilnikov, L., Shilnikov, A., Turaev, D., Chua, L.: Methods of Qualitative Theory in Nonlinear Dynamics, Part 1. World Scientific Publishing Co. Pte. Ltd., Singapore (1998)
34. Zhang, X., Chen, L.: The periodic solution of a class of epidemic models. Comput. Math. Appl. **38**, 61–71 (1999)
35. Hassard, B., Kazarinoff, N., Wan, Y.: Theory and Applications of Hopf Bifurcation. Cambridge University Press, Cambridge (1981)
36. Kumar, S., Srivastava, S., Chingakham, P.: Hopf bifurcation and stability analysis in a harvested one-predator–two-prey model. Appl. Math. Comput. **129**, 107–118 (2002)
37. Allison, E., Coltobetal, A.: A mathematical model of the effector cell response to cancer. Math. Comput. Model. **39**, 1313–1327 (2004)